Journal of Clinical Monitoring and Computing (2019) 33:85–94
https://doi.org/10.1007/s10877-018-0136-1

ORIGINAL RESEARCH

Assessment of cerebral hemodynamic parameters using pulsatile versus non-pulsatile cerebral blood outflow models

Agnieszka Uryga[1] · Magdalena Kasprowicz[1] · Leanne Calviello[2] · Rolf R. Diehl[3] · Katarzyna Kaczmarska[4,5] · Marek Czosnyka[2,5]

Received: 1 February 2018 / Accepted: 29 March 2018 / Published online: 4 April 2018

Abstract

Background Prior methods evaluating the changes in cerebral arterial blood volume (ΔC_aBV) assumed that brain blood transport distal to big cerebral arteries can be approximated with a non-pulsatile flow (CFF) model. In this study, a modified ΔC_aBV calculation that accounts for pulsatile blood flow forward (PFF) from large cerebral arteries to resistive arterioles was investigated. The aim was to assess cerebral hemodynamic indices estimated by both CFF and PFF models while changing arterial blood carbon dioxide concentration ($EtCO_2$) in healthy volunteers.

Materials and methods Continuous recordings of non-invasive arterial blood pressure (ABP), transcranial Doppler blood flow velocity ($CBFV_a$), and $EtCO_2$ were performed in 53 young volunteers at baseline and during both hypo- and hypercapnia. The time constant of the cerebral arterial bed (τ) and critical closing pressure (CrCP) were estimated using mathematical transformations of the pulse waveforms of ABP and $CBFV_a$, and with both pulsatile and non-pulsatile models of ΔC_aBV estimation. Results are presented as median values ± interquartile range.

Results Both CrCP and τ gave significantly lower values with the PFF model when compared with the CFF model ($p \ll 0.001$ for both). In comparison to normocapnia, both CrCP and τ determined with the PFF model increased during hypocapnia [$CrCP_{PFF}$ (mm Hg): 5.52 ± 8.78 vs. 14.36 ± 14.47, $p = 0.00006$; τ_{PFF} (ms): 47.4 ± 53.9 vs. 72.8 ± 45.7, $p = 0.002$] and decreased during hypercapnia [$CrCP_{PFF}$ (mm Hg): 5.52 ± 8.78 vs. 2.36 ± 7.05, $p = 0.0001$; τ_{PFF} (ms): 47.4 ± 53.9 vs. 29.0 ± 31.3, $p = 0.0003$]. When the CFF model was applied, no changes were found for CrCP during hypercapnia or in τ during hypocapnia.

Conclusion Our results suggest that the pulsatile flow forward model better reflects changes in CrCP and in τ induced by controlled alterations in $EtCO_2$.

Keywords Transcranial Doppler ultrasound · Cerebral arterial blood volume · Cerebral arterial compliance · Time constant of cerebral arterial bed · Critical closing pressure · Hypercapnia · Hypocapnia

✉ Agnieszka Uryga
agnieszka.uryga@pwr.edu.pl

[1] Department of Biomedical Engineering, Faculty of Fundamental Problems of Technology, Wroclaw University of Science and Technology, Wybrzeze Wyspianskiego 27, 50-370 Wroclaw, Poland

[2] Brain Physics Laboratory, Department of Clinical Neurosciences, Division of Neurosurgery, University of Cambridge, Cambridge, UK

[3] Department of Neurology, Alfried-Krupp-Krankenhaus, Essen, Germany

[4] Department of Neurosurgery, Mossakowski Medical Research Centre Polish Academy of Sciences, Warsaw, Poland

[5] Institute of Electronic Systems, Warsaw University of Technology, Warsaw, Poland

1 Introduction

Changes in cerebral arterial blood volume (ΔC_aBV) stored in conductive cerebral arteries are determined by interactions between pulsatile cerebral arterial inflow and flow forward, i.e. through the resistive arteries (mainly arterioles). Previous experimental methodology utilizing magneto-flowmetry was proposed for the assessment of the ΔC_aBV, with cerebral blood flow measured in the vertebral arteries of anesthetized dogs [1]. Scientists have followed up with magnetic resonance imaging (MRI) phase-coded evaluation [2, 3]. However, MRI as an advanced imaging technique is expensive, and allows only for a 'snapshot' evaluation of ΔC_aBV. Recently, we proposed a methodology for estimating ΔC_aBV using non-invasive, inexpensive

transcranial Doppler ultrasonography (TCD). TCD allows for the continuous investigation of ΔC_aBV at the patient's bedside [4, 5], presuming that pulsatile inflow into a system of vascular compartmental compliances produces an extension of ΔC_aBV, while flow forward can be approximated by continuous flow. This has been termed the 'continuous flow forward' (CFF) model [4].

In the current study, an important modification of ΔC_aBV estimation has been suggested that invites an alternative analysis of cerebral arterial compliance considering pulsatile blood flow forward (a simplified model of the cerebral blood circulation is presented in Fig. 1)—termed the 'pulsatile flow forward' (PFF) model. The estimation of ΔC_aBV drives the calculation of a set of parameters describing cerebral hemodynamics [6] such as cerebral arterial compliance (C_a) [4, 5], the cerebral arterial time constant (τ) [7–9], and critical closing pressure (CrCP) [10].

Model-based hemodynamic parameters have been reported to be promising clinical indices. The τ was found shorter during cerebral vasospasm (CVS) after subarachnoid hemorrhage (SAH), and these changes precede the increase of mean blood flow velocity in the middle cerebral artery. Thus, the τ may serve as an early-warning indicator of CVS [11]. Furthermore, the τ was used to monitor the impairment of cerebrovascular reactivity in internal carotid artery occlusive disease, which may indicate an increased risk of cerebral ischemia [9]. The decrease in C_a was found to be correlated with the severity of the internal carotid artery disease [12]. The CrCP was reported to be associated with unfavourable outcome in patients with CVS after SAH [13] and was also successfully used for non-invasive estimation of cerebral perfusion pressure in patients after traumatic brain injury (TBI) [14]. The cerebral hemodynamic indices can also be useful when studying the physiology of hemodynamic events. For example, the development of the method for continuous ΔC_aBV estimation enable us to determine that the main parameter shaping the intracranial pulse waveform in TBI patients is the pulse amplitude of ΔC_aBV [15].

Here, we compared the hemodynamic parameters estimated by both the CFF and PFF models while manipulating arterial blood carbon dioxide concentration in healthy volunteers.

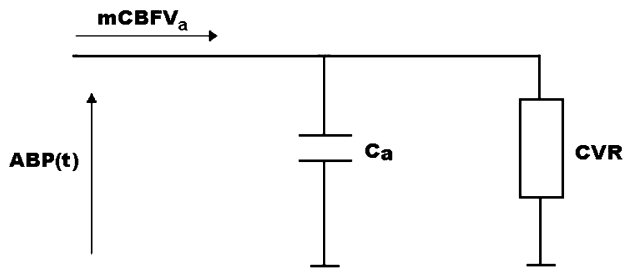

Fig. 1 Simplified model of cerebral blood flow circulation. In the pulstile flow foward model (PFF), the inflow pulse (inflow to C_a/CVR vascular impedance) and the outflow down CVR, which is ABP(t)/CVR are considered. *mCBFV$_a$* cerebral blood flow velocity in the middle cerebral artery, *ABP(t)* arterial blood pressure, *CVR* cerebrovascular resistance and *C_a* the compliance of the cerebral arterial bed

2 Materials and methods

2.1 Subjects

Fifty-three healthy volunteers (31 females and 22 males, median age: 22, range: 18–31 years) were recruited via advertisements posted on the website of the Wroclaw University of Science and Technology. The exclusion criteria included: tobacco smokers, incidence of cardiovascular, respiratory or neurological diseases, chronic illness, being on treatment or therapy known to alter cardiovascular parameters, and vascular risk factors (i.e. hypertension, diabetes mellitus, dyslipidaemia, etc.). Subjects were asked to avoid caffeine and alcohol for 12 h before the TCD measurements were taken. All participants went through a basic medical examination to further exclude any disorders.

2.2 Protocol and data acquisition

The middle cerebral artery (MCA) was insonated using TCD (Doppler BoxX, DWL, Compumedics Germany GmbH, Singen, Germany) to non-invasively measure the cerebral blood flow velocity ($CBFV_a$). The anatomical segments of the MCA were identified by their depth and the Doppler spectra. The ultrasound 2 MHz probe was attached to a plastic helmet and immobilized by fitting the measuring frame to the patient's head. The level of carbon dioxide released at the end of expiration ($EtCO_2$) was recorded with a fitted mask applied to the patient's nose and mouth and connected to a capnograph (RespSense™, NONIN, Plymouth, MN, USA) via a sample line. The beat-to-beat arterial blood pressure (ABP) signal was measured non-invasively using photoplethysmography (Finometer MIDI, FMS Medical Systems, Amsterdam, The Netherlands). The measuring cuff was placed on the middle finger of the left hand, which was held at the level of the heart. Electrocardiogram (ECG) signals were recorded by a three-lead surface electrode device, attached to the Finometer MIDI device. According to experimental protocol, during the measurements, all participants were seated in the middle of the chair with feet flat on the floor. First, 5 min of spontaneous breathing were recorded (normocapnia). Afterwards, participants were asked to re-breathe from a plastic reservoir bag attached to the face mask, until the concentration of $EtCO_2$ was at least 45 mm Hg and had reached a plateau (hypercapnia)—see

Fig. 2. In this state, signals were recorded within approximately 5 min. In the last step, the plastic sack was removed, and volunteers were asked to breathe deeply for a maximum of 5 min to achieve mild hypocapnia.

2.3 Signal analysis

Recorded signals were sampled with a frequency of 200 Hz. Data was collected and further analyzed using the Intensive Care Monitor (ICM+) system (Cambridge Enterprise Ltd., Cambridge, UK). All recorded signals were visually inspected to identify artefacts and noise. All recognized distortions were removed manually, and further analysis was performed with utilization of the correct parts of the signals.

2.4 Pulsatile changes in cerebral blood volume

The amount of arterial blood supplied to the cerebral space by the vascular system during a cardiac cycle is partially compensated by the simultaneous outflow of blood through the venous system. Both the cerebral blood inflow (CBF_{in}) and the cerebral blood outflow (CBF_{out}) have a pulsatile character, but their pulse waveform shapes are different, resulting in ΔC_aBV during a heartbeat. The interaction between pulsatile changes in CBF_{in} and CBF_{out} determines the transient, time-dependent ΔC_aBV, and can be described by the following equation (Avezaat and van Eijndhoven 1986):

$$\Delta C_aBV(t) = \int_{t_0}^{t} \left(CBF_{in}(s) - CBF_{out\,(s)}\right)ds \quad (1)$$

where t_0 is the beginning, t is the end of single cardiac cycle, and s is the variable of integration. When employing TCD, CBF_{out} cannot be monitored simultaneously with CBF_{in}. Therefore, in our previous papers which used the CFF model [4, 5, 8, 9], we assumed that CBF_{outCFF}, which has a low pulsatility in relation to CBF_{in} [16], could be approximated by a continuous flow that is equal to the cerebral arterial inflow (CBF_a) averaged over a period longer than one cardiac cycle. In practice, a time interval lasting at least 6 s was considered [17, 18].

$$CBF_{outCFF}(t) = meanCBF_a \quad (2)$$

Applying this modification to Eq. 1, we determined a definition of ΔC_aBV during a one cardiac cycle, estimated with the CFF model (ΔC_aBV_{CFF}):

$$\Delta C_aBV_{CFF}(t) = \int_{t_0}^{t} (CBF_a(s) - meanCBF_a)ds \quad (3)$$

where t_0 is the beginning, t is the end of single cardiac cycle, and s is the variable of integration. However, as mentioned

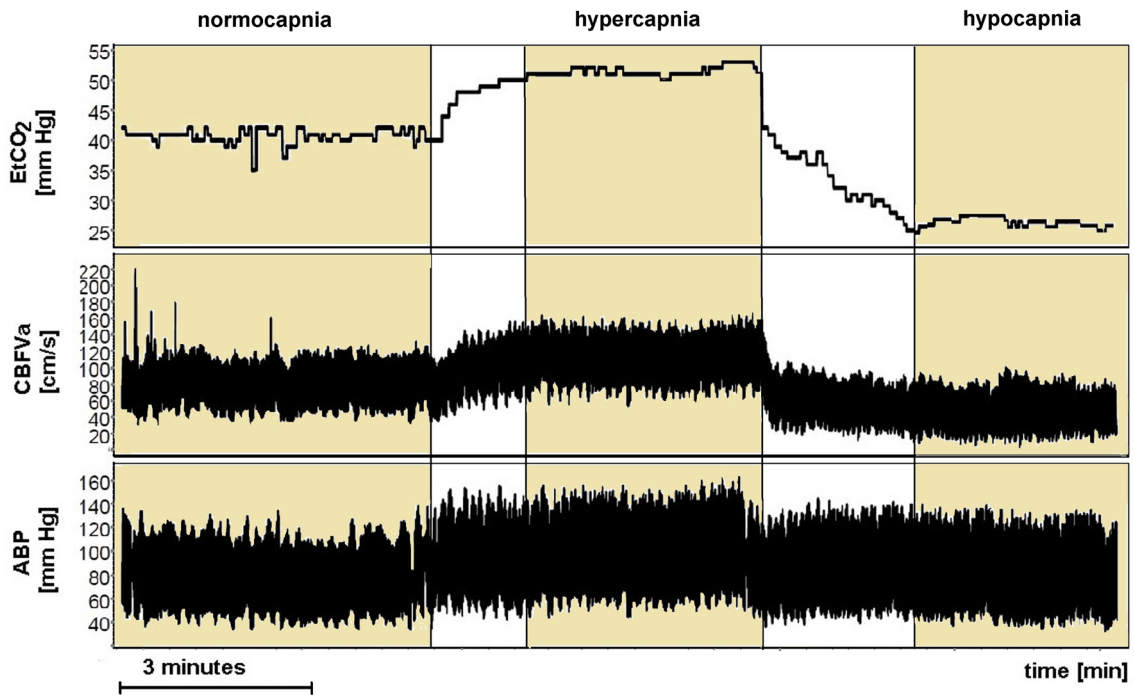

Fig. 2 Continuous monitoring of end-tidal CO_2 ($EtCO_2$), cerebral blood flow velocity in the middle cerebral artery ($CBFV_a$) and arterial blood pressure (ABP) during normo-, hyper- and hypocapnia in a 24-year-old male volunteer

above, the blood outflow is not constant and depends on the impedance of the afferent part of the vascular system controlled by the vasomotor tone of the cerebral vessels and pulsatile changes in ABP. Therefore, the cerebral blood outflow (CBF_{outPFF}) was alternatively modelled as ABP divided by the cerebrovascular resistance (CVR):

$$CBF_{outPFF}(t) = \frac{ABP(t)}{CVR} \tag{4}$$

CVR was determined as a ratio between pressure and cerebral blood flow. However, in the formula below (Eq. 5), CVR was normalized [cerebral blood flow was divided by the unknown cross-sectional area (S_a)]. Then, CVR was estimated as a ratio between mean ABP and mean $CBFV_a$ as follows [4, 6]:

$$CVR = \frac{meanABP}{meanCBFV_a}\left(\frac{mmHg\ s}{cm}\right) \tag{5}$$

Thus, by applying Eqs. 4 and 5 to Eq. 1, the ΔC_aBV during a one cardiac cycle was estimated with the PFF model (ΔC_aBV_{PFF}):

$$\Delta C_aBV(t)_{PFF} = \int_{t_0}^{t}\left(CBF_a(s) - \frac{ABP(s)}{CVR}\right)ds \tag{6}$$

where t_0 is the beginning, t is the end of single cardiac cycle, and s is the variable of integration.

Assuming that the S_a of the insonated vessel remains constant in healthy subjects [4, 19, 20], and taking into account a finite sampling frequency, Eqs. 3 and 6 can be rewritten utilizing TCD-determined $CBFV_a$:

$$\Delta C_aBV(n)_{CFF} = \sum_{i=1}^{n}[CBFV_a(i) - meanCBFV_a(i)]\Delta t(i) \times S_a\left(\frac{cm}{s}\ s\ cm^2\right) \tag{7}$$

$$\Delta C_aBV(n)_{PFF} = \sum_{i=1}^{n}\left[CBFV_a(i) - \frac{ABP(i)}{CVR}\right]\Delta t(i) \times S_a\left(\frac{cm}{s}\ s\ cm^2\right) \tag{8}$$

where n is the following number of samples from the beginning of one cardiac cycle, Δt is the time interval between two consecutive samples, $CBFV_a(i)$—a moving average of the $CBFV_a$ from the window including several previous heart cycles (in our study a 6-s window was applied), ABP(i)—arterial blood pressure at each time, CVR—a moving average of cerebrovascular resistance, and S_a denoting an unknown cross-sectional area of the insonated vessel. Note that both ΔC_aBV_{CFF} and ΔC_aBV_{PFF} are normalized for calculation (divided into unknown cross-sectional area, S_a). Thus, the units of ΔC_aBV_{CFF} and ΔC_aBV_{PFF} and their amplitudes are not units of volume (cm^3), but (cm). Both signals obtained from the above calculations (ΔC_aBV_{CFF} and ΔC_aBV_{PFF}) have clearly pulsatile components, but the shape of the ΔC_aBV_{PFF} waveform is different and its amplitude is lower than that of ΔC_aBV_{CFF}—see Fig. 3.

2.5 Model-based parameters of cerebrovascular dynamics

The two methods for describing changes in cerebral arterial blood volume calculation (ΔC_aBV_{CFF} and ΔC_aBV_{PFF}) were used for the estimation of indices describing cerebrovascular dynamics including: cerebral arterial compliance (C_a), the cerebral arterial time constant (τ), and critical closing pressure (CrCP). The algorithms for the calculations of these cerebrovascular model-based indices were presented in detail elsewhere [4, 9, 10] and briefly described below.

2.6 Compliance of the cerebral arterial bed

Compliance describes the ability of the cerebral vessels to distend and increase in volume with increasing pressure [21]. The C_a is here defined as a ratio between the pulsatile amplitude of ΔC_aBV ($Amp\Delta C_aBV$) and the amplitude of ABP (AmpABP) [4, 5]. Note that in the formulas below (Eqs. 9–11), C_a was normalized [divided by the unknown cross-sectional area (S_a)]. Then, C_a was expressed as:

$$C_a = \frac{Amp\Delta C_aBV}{AmpABP}\quad\left(\frac{cm}{mmHg}\right) \tag{9}$$

Using the CFF model of the compliance of the cerebral arterial bed (C_{aCFF}) was calculated as:

$$C_{aCFF} = \frac{Amp\Delta C_aBV_{CFF}}{AmpABP}\quad\left(\frac{cm}{mmHg}\right) \tag{10}$$

where $Amp\Delta C_aBV_{CFF}$ and AmpABP were determined, using Fourier transform, as the amplitudes of fundamental components of ΔC_aBV_{CFF} and ABP, respectively.

The following equation was applied to estimate the compliance of the cerebral arterial bed using the PFF model (C_{aPFF}):

$$C_{aPFF} = \frac{Amp\Delta C_aBV_{PFF}}{AmpABP}\quad\left(\frac{cm}{mmHg}\right) \tag{11}$$

where $Amp\Delta C_aBV_{PFF}$ was estimated using the Fourier transform of changes in ΔC_aBV_{PFF} during a cardiac cycle as follows:

$$Amp\Delta C_aBV_{PFF} = \left(AmpCBFV_a - \frac{AmpABP}{CVR}\right)\Big/2\pi \cdot HR\quad(cm) \tag{12}$$

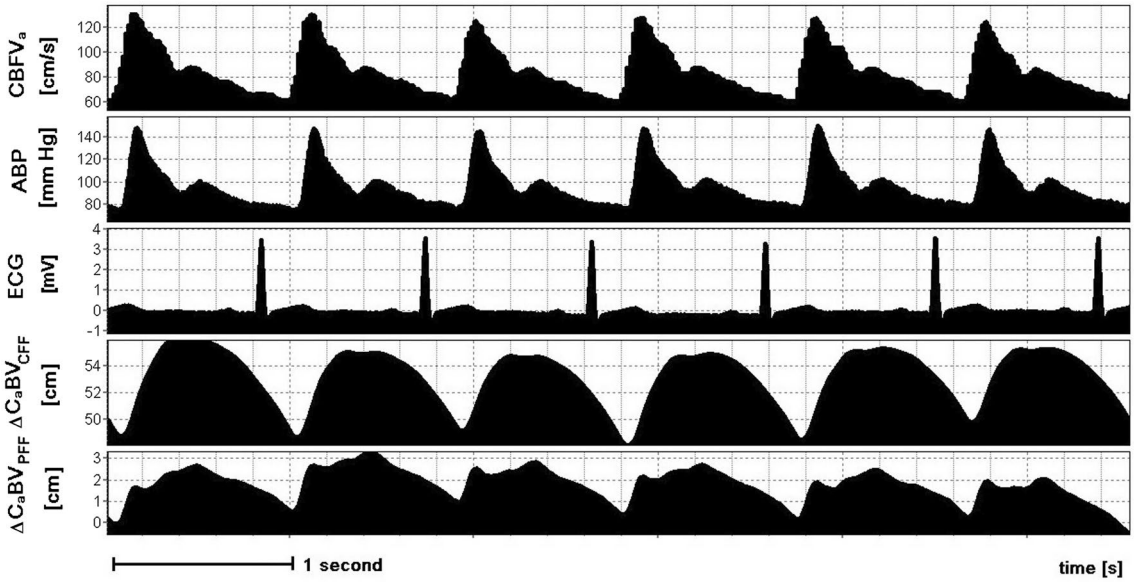

Fig. 3 Pulsatile changes in cerebral blood flow velocity ($CBFV_a$), arterial blood pressure (ABP), electrocardiogram (ECG), and changes in cerebral arterial blood volume (ΔC_aBV) calculated using both the continuous flow forward (CFF) and the pulsatile flow forward (PFF) models during normocapnia in a 24-year-old male volunteer. ΔC_aBV is normalized by the cross-sectional area of the insonated vessel. Results obtained with the PFF model include the influence of cerebrovascular resistance and the pulsatile character of ABP, whereas the CFF model is based on mean $CBFV_a$

The heart rate (HR) was defined as the fundamental frequency of ABP and expressed in (Hz). Equation 12 was introduced in a new proposal of C_{aPFF} estimation to account for the time delay between signals recorded from cerebral arteries using transcranial Doppler ultrasonography ($CBFV_a$) and from the finger using photoplethysmography (ABP), under the assumption that the 'physiological' phase shift between the first harmonics of $CBFV_a(t)$ and ABP(t) pulses is small and constant.

2.7 Time constant of the cerebral arterial bed

The time constant of the cerebral arterial bed (τ) can be interpreted as the time required to fill the arterial bed distal to the level of the insonated vessel. To calculate τ, we used a simplified model of cerebral blood flow circulation [18] consisting of a single resistor and capacitor, representing CVR, and C_a, respectively—see Fig. 1. The τ was then calculated, analogous to an electrical resistor–capacitor (RC) circuit, as the product of C_a and CVR [7, 8]:

$$\tau = C_a \cdot CVR \quad (s) \tag{13}$$

where CVR was estimated according to Eq. 5, whereas to calculate C_a either Eq. 10 or Eq. 11 was used, giving two estimates: a CFF—based time constant (τ_{CFF}) and a PFF—based time constant (τ_{PFF}). Note that the product of C_a and CVR removes the unknown contribution from the cross-sectional area (normalization is not required), therefore τ can be expressed in units of time (seconds).

2.8 Critical closing pressure

Critical closing pressure (CrCP) is defined as the level of arterial pressure below which arterial vessels start to collapse [22]. In this study, we used a multi-parameter model of CrCP calculation proposed by Varsos et al. [10]:

$$CrCP = meanABP - \frac{meanABP}{\sqrt{(CVR \cdot C_a \cdot HR \cdot 2\pi)^2 + 1}} \quad (mmHg) \tag{14}$$

Two estimators of C_a (Eq. 10 or Eq. 11) were applied to Eq. 14, giving two definitions: CFF—based critical closing pressure ($CrCP_{CFF}$) and PFF—based critical closing pressure ($CrCP_{PFF}$). Similar to τ, the unknown cross-sectional area is reduced, and both estimators of CrCP are calculated with the 'physical' unit mm Hg.

2.9 Statistical methods

The normality of the analyzed data distribution was evaluated by a Kruskal–Wallis test with a Lilliefors correction. The hypothesis of normality was rejected for most of the analyzed parameters, therefore non-parametric tests were used. Median values of hemodynamic indices estimated

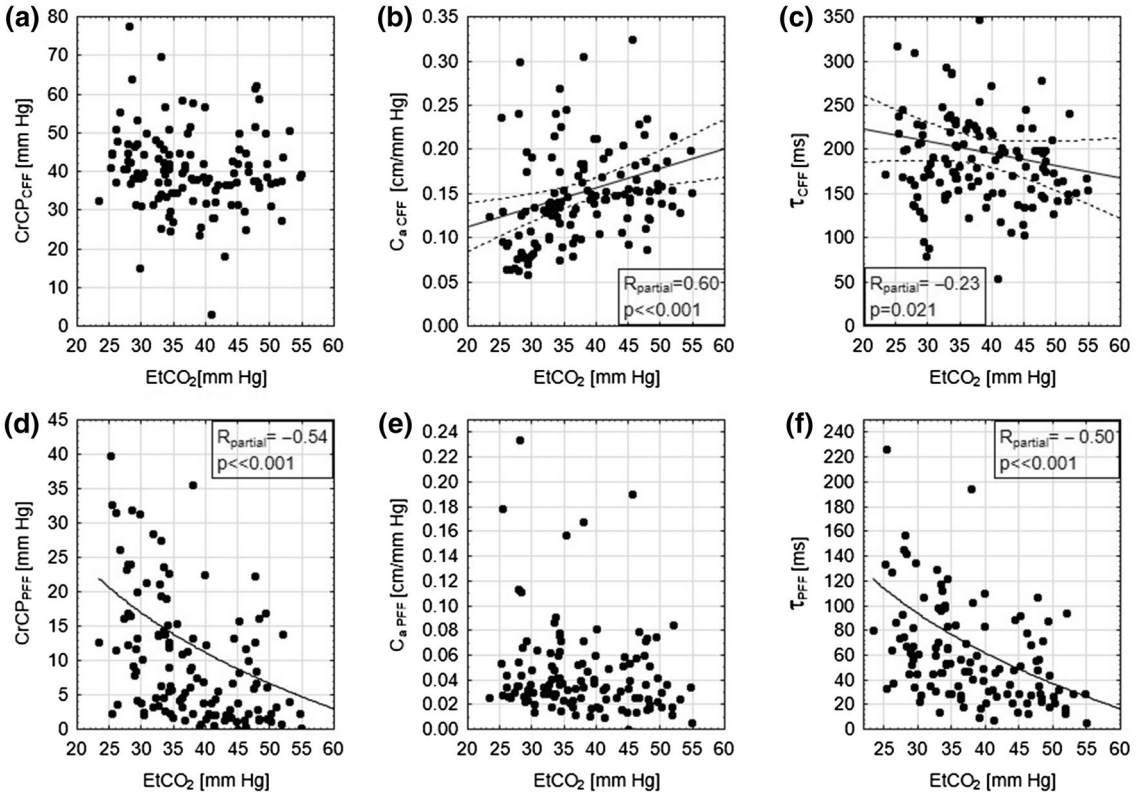

Fig. 4 The correlations for pooled data between: critical closing pressure (CrCP), compliance of the cerebral arterial bed (C_a), and the time constant of cerebral arterial bed (τ) calculated using the continuous flow forward model (CFF, **a**–**c**) and the pulsatile flow forward model (PFF, **d**–**f**) and end–tidal carbon dioxide concentration ($EtCO_2$). In Panels **b** and **c**, the solid line is the linear fit and the dashed line is a 95% confidence interval, whereas in **d** and **f**, the solid line is exponentially fitted as determined by the least squares method

using both CFF and PFF models were compared using a Wilcoxon signed-rank post-hoc test. In order to evaluate differences between physiological parameters (ABP, $EtCO_2$, $CBFV_a$, HR) and hemodynamic indices during normo-, hyper-, and hypocapnia, a nonparametric ANOVA Friedman's test was applied. Differences between two particular $EtCO_2$ changes (either hypocapnia or hypercapnia in relation to normocapnia) were analyzed using a Wilcoxon signed-rank post-hoc test with a Bonferroni adjustment. The relationships between $EtCO_2$ and cerebrovascular indices were calculated using multiple linear or linearized regression analyses with subjects treated as categorical factors using dummy variables (with respect to the inter-subject variability) and a partial coefficient ($R_{partial}$) between analyzed variables, as recommended by Bland and Altman [23, 24]. The level of significance for the ANOVA Friedman's test was set at 0.05 and at $p_{post\text{-}hoc} < 0.025$ for post-hoc comparison. Results are presented as medians (interquartile ranges (IQR), 25th–75th percentile). STATISTICA (data analysis software system), version 12 (StatSoft, Inc., Tulsa, USA) was used to perform the statistical analysis.

3 Results

3.1 Comparison of hemodynamic parameters at baseline

Estimators calculated using the CFF and PFF models differ quantitatively—see Table 2.

C_a, τ, and CrCP were lower in value when estimated using the PFF model ($p \ll 0\,0.001$ for all differences).

3.2 Physiological variables during $EtCO_2$ changes

Median values (25th–75th percentile) of ABP, $EtCO_2$, HR, and $CBFV_a$ along with the results of statistical comparisons between either hypocapnia or hypercapnia in relation to normocapnia are presented in Table 1. Changes of $EtCO_2$ have a meaningful effect on all of the analyzed physiological parameters (Friedman ANOVA $p \ll 0.001$ for all differences). During hypercapnia, $CBFV_a$, HR,

Table 1 Median values (25th–75th percentile) of physiological parameters for 53 volunteers during hypo-, normo- and hypercapnia

Parameter	Hypocapnia	Normocapnia	Hypercapnia	*p* value normocapnia vs. hypocapnia	*p* value normocapnia vs. hypercapnia
$CBFV_a$ (cm/s)	50.6 (43.9–55.6)	71.9 (63.3–78.2)	91.6 (80.4–106.7)	≪0.001	≪0.001
ABP (mmHg)	91.1 (81.9–97.5)	89.3 (79.9–98.5)	98.8 (87.6–109.5)	n.s	≪0.001
AmpABP (mmHg)	14.5(12.6–16.7)	13.1(11.4–14.9)	14.8(12.6–17.2)	≪0.001	≪0.001
$EtCO_2$ (mmHg)	29.4 (27.9–32.5)	36.3 (33.6–39.0)	47.5 (44.6–49.5)	≪0.001	≪0.001
HR (beats/min)	85.7 (79.1–96.0)	73.4 (68.4–81.7)	76.9 (69.6–84.9)	≪0.001	≪0.001

$CBFV_a$ cerebral blood flow velocity in the middle cerebral artery, *ABP* arterial blood pressure, *AmpABP* amplitude of pulsatile changes in ABP, *$EtCO_2$* end-tidal carbon dioxide concentration, and *HR* heart rate

p values of the Friedman ANOVA were lower than 0.001 for all parameters

Table 2 Median values (25th–75th percentile) of hemodynamic parameters calculated using both continuous (CFF) and pulsatile (PFF) flow forward models for 53 volunteers during hypo-, normo- and hypercapnia

Parameter	Hypocapnia	Normocapnia	Hypercapnia	*p* value normocapnia vs. hypocapnia	*p* value normocapnia vs. hypercapnia
$Amp\Delta C_aBV_{CFF}$ (cm)	1.5 (1.2–1.7)	2.0 (1.7–2.3)	2.2 (1.9–2.7)	≪0.001	≪0.001
$Amp\Delta C_aBV_{PFF}$ (cm)	0.56 (0.40–0.77)	0.48 (0.28–0.72)	0.41 (0.28–0.63)	n.s	n.s
CVR (mmHg s/cm)	1.8 (1.6–2.1)	1.3 (1.1–1.5)	1.1 (0.9–1.3)	≪0.001	≪0.001
C_{aCFF} (cm/mmHg)	0.099 (0.079–0.131)	0.154 (0.133–0.191)	0.153 (0.142–0.187)	≪0.001	n.s
C_{aPFF} (cm/mmHg)	0.035 (0.027–0.048)	0.038 (0.024–0.063)	0.031 (0.018–0.054)	n.s	0.023
τ_{CFF} (ms)	190.0 (160.4–222.1)	204.2 (168.0–233.6)	173.2 (145.8–198.7)	n.s	≪0.001
τ_{PFF} (ms)	72.8 (52.5–98.2)	47.4 (28.7–82.6)	29.0 (20.0–51.3)	0.002	0.0003
$CrCP_{CFF}$ (mmHg)	42.4 (34.5–48.0)	38.2 (31.4–42.4)	37.6 (32.2–43.0)	0.0001	n.s
$CrCP_{PFF}$ (mmHg)	14.36 (8.31–22.78)	5.52 (3.02–11.80)	2.36 (1.26–8.30)	0.00006	0.0001

$Amp\Delta C_aBV$ amplitude of cerebral arterial blood volume, *CVR* cerebrovascular resistance, C_a compliance of cerebral arterial bed, τ cerebral arterial time constant, *CrCP* critical closing pressure

p values of Friedman ANOVA were lower than 0.001 for all parameters except for $Amp\Delta C_aBV_{PFF}$ (not significant) and C_{aPFF} ($p = 0.002$)

ABP, and ABP pulse amplitude significantly increased in comparison with normocapnia. On the other hand, hypocapnia caused significant decreases in $EtCO_2$ and $CBFV_a$, and an increase in HR in relation to normocapnia. The elevation of ABP during hypocapnia was statistically insignificant, but the pulse amplitude of ABP showed a significant increase.

3.3 Hemodynamic indices estimated using CFF and PFF models during $EtCO_2$ changes

When the PFF model was applied, hypercapnia shortened τ_{PFF} and decreased $CrCP_{PFF,}$ whereas hypocapnia induced the opposite changes, see Table 2. A clear reaction to alterations in $EtCO_2$ was not noticed when the CFF

model was used. Elevated $EtCO_2$ did not affect $CrCP_{CFF,}$ nor did a decrease in $EtCO_2$ influence τ_{CFF} (see Table 2). However, similar to parameters calculated with the PFF model, $CrCP_{CFF}$ increased during hypocapnia, whereas τ_{CFF} decreased during hypercapnia when compared to normocapnia. In our study sample, hypocapnia increased CVR and decreased $C_{aCFF,}$ but did not change C_{aPFF}. In contrast, hypercapnia decreased CVR, did not change $C_{aCFF,}$ and slightly decreased C_{aPFF}. When the CFF model was used to estimate the amplitude of ΔC_aBV ($Amp\Delta C_aBV$), some significant differences were shown during hypocapnia and hypercapnia: $Amp\Delta C_aBV_{CFF}$ decreased during $EtCO_2$ reduction and increased during $EtCO_2$ elevation (see Table 2), whereas the amplitude of ΔC_aBV estimated with the PFF model, was not affected by changes in $EtCO_2$.

3.4 Correlations between PFF and CFF estimators and $EtCO_2$

The analysis of pooled data at all $EtCO_2$ levels (normo-, hyper- and hypocapnia) showed a positive, robust relationship between $EtCO_2$ and C_{aCFF} ($R_{partial} = 0.60$, $p \ll 0.001$), but no correlation was found between $EtCO_2$ and C_{aPFF}. On the other hand, $CrCP_{PFF}$ was negatively correlated with $EtCO_2$ ($R_{partial} = -0.54$, $p \ll 0.001$), but not correlated with $CrCP_{CFF}$. The τ_{CFF} was negatively and weakly correlated with $EtCO_2$ ($R_{partial} = -0.23$, $p = 0.001$), whereas τ_{PFF} was negatively correlated with $EtCO_2$ ($R_{partial} = -0.50$, $p \ll 0.001$). Figure 4 provides a visual representation of these statistics.

4 Discussion

In this study, we compared hemodynamic indices estimated using both CFF and PFF models during $EtCO_2$ changes in normal subjects. A group evaluation showed that hypercapnia reduced C_a estimated with the PFF model but did not affect C_a determined with the CFF model. Either the reduction or no change in C_a during hypercapnia seemed to be counterintuitive at first, as carbon dioxide is a known vasodilator and an increase in C_a is expected when $EtCO_2$ is elevated. In our study, however, hypercapnia caused a concomitant increase in mean ABP and its amplitude. As a result, the amplitude of the ΔC_aBV signal calculated using the CFF model increased, whereas it remained unchanged when the PFF model was applied. Consequently, C_a (being the ratio between $Amp\Delta C_aBV$ and AmpABP) did not change when estimated using the CFF model but decreased during hypercapnia when calculated using the PFF model. These differences in C_a estimation influenced other hemodynamic indices that included C_a in their calculations, namely τ and CrCP. The τ estimated with both models shortened during hypercapnia. Shorter τ during $EtCO_2$ elevation suggests a decrease in wall tension, and should lead to a decrease in CrCP due to vasodilatation [25]. A significant decrease in $CrCP_{PFF}$ was observed, however no change in $CrCP_{CFF}$ was found during hypercapnia.

During hypocapnia, a decrease in C_a was expected as a consequence of increasing CVR [5]. C_a estimated with the CFF model, indeed demonstrated a significant decrease resulting from a reduction of $Amp\Delta C_aBV_{CFF}$ and an increase in AmpABP. On the contrary, there was no change in C_a estimated with the PFF model despite an increase in AmpABP and with $Amp\Delta C_aBV_{PFF}$ remaining constant. Therefore, τ (being a product of C_a and CVR) estimated with the PFF model increased during hypocapnia, but did not change when the CFF model was applied. This lack of variation in τ_{CFF} resulted from the significant increase in HR during the $EtCO_2$ decrease seen in our current data. In a previous study, performed in another cohort of normal subjects, HR remained unchanged during hypocapnia, and a significant prolongation of τ estimated with the CFF model was observed [9]. During hypocapnia, CrCP estimated with both models increased, demonstrating the expected response to an $EtCO_2$ decrease. It should be noted that in contrast to τ, the mathematical formula for CrCP estimation accounts for HR changes.

Another difference found when the PFF and CFF models were compared is that the values of the hemodynamic indices calculated using the PFF model are significantly lower than those estimated using the CFF model. All observed differences in results obtained with both models are related to the fact that the PFF model includes the influence of CVR and the pulsatile character of ABP, whereas the CFF model is based on the mean value of $CBFV_a$.

4.1 Limitations of the study

There is no agreement on whether partial pressure of carbon dioxide ($PaCO_2$) alterations significantly affect MCA diameter and influence TCD—based ΔC_aBV estimates [26, 27]. Based on current research, using angiography [28] and MRI [29], we assumed that during moderate $PaCO_2$ alterations, that the M1 segment of the MCA under steady-state hemodynamic conditions retains relatively constant diameter [19, 20, 30]. However, conflicting results have recently been published [31, 32]. Thus, TCD—based hemodynamic parameters need to be carefully interpreted during $PaCO_2$ changes, and further investigation in this area is required by using neuroimaging techniques with both high temporal and spatial resolution.

We have not validated our results with MRI due to the high costs of MRI study, and due to the fact that our measurements were conducted in laboratory settings in healthy, young volunteers without medical indications for MRI

examination. Although MRI is a non-invasive measurement, it requires an intravascular contrast agent to quantify $\Delta C_a BV$ [33]. Nevertheless, we are aware that comparing our results with MRI outcome would provide valuable information about the proposed method for $\Delta C_a BV$ estimation, therefore MRI validation will be a goal of our further studies.

5 Conclusion

There are two possible ways to estimate hemodynamic parameters: using pulsatile and continuous flow forward (PFF and CFF, respectively). Critical closing pressure and the cerebrovascular time constant (τ) are lower for the PFF than for the CFF model. Hemodynamic indices calculated using the PFF model demonstrated more clear reactions to changes in $EtCO_2$ than those determined with the CFF model.

Acknowledgements We thank Krystian Gruszczyński, Msc. Eng. for assistance with data collection and Tomasz Szczepański, PhD for reviewing medical history and physical examination.

Funding This research was supported by the National Science Center (Poland) under Grant No. UMO-2013/10/E/ST7/00117.

Compliance with ethical standards

Conflict of interest ICM + Software is licensed by Cambridge Enterprise, Cambridge, UK, http://www.neurosurg.cam.ac.uk/icmplus/. Prof. Czosnyka has a financial interest in a fraction of the licensing fee for ICM + software. The other authors declare that they have no conflicts of interest.

Informed consent The protocol complied with the Declaration of Helsinki of the World Medical Association, and all participants gave written informed consent before participating in the study.

Research involving human and animal rights The study was approved by the bioethical committee of the Wroclaw Medical University (Permission No. KB-170/2014).

References

1. Avezaat CJJ, van Eijndhoven JHM. The role of the pulsatile pressure variations in intracranial pressure monitoring. Neurosurg Rev. 1986;9:113–20.
2. Alperin N, Sivaramakrishnan A, Lichtor T. Magnetic resonance imaging-based measurements of cerebrospinal fluid and blood flow as indicators of intracranial compliance in patients with Chiari malformation. J Neurosurg. 2005;103:46–52.
3. Stoquart-Elsankari S, Lehmann P, Villette A, Czosnyka M, Meyer M-E, Deramond H, et al. A phase-contrast MRI study of physiologic cerebral venous flow. J Cereb Blood Flow Metab. 2009;29:1208–15.
4. Kim DJ, Kasprowicz M, Carrera E, Castellani G, Zweifel C, Lavinio A, et al. The monitoring of relative changes in compartmental compliances of brain. Physiol Meas. 2009;30:647–59.
5. Carrera E, Kim DJ, Castellani G, Zweifel C, Smielewski P, Pickard JD, et al. Effect of hyper- and hypocapnia on cerebral arterial compliance in normal subjects. J Neuroimaging. 2011;21:121–5.
6. Nasr N, Czosnyka M, Pavy-Le Traon A, Custaud M-A, Liu X, Varsos GV, et al. Baroreflex and cerebral autoregulation are inversely correlated. Circ J. 2014;78:2460–7.
7. Czosnyka M, Richards HK, Reinhard M, Steiner L, Budohoski K, Smielewski P, et al. Cerebrovascular time constant: dependence on cerebral perfusion pressure and end-tidal carbon dioxide concentration. Neurol Res. 2012;34:17–24.
8. Kasprowicz M, Diedler J, Reinhard M, Carrera E, Steiner LA, Smielewski P, et al. Time constant of the cerebral arterial bed in normal subjects. Ultrasound Med Biol. 2012;38:1129–37.
9. Kasprowicz M, Diedler J, Reinhard M, Carrera E, Smielewski P, Budohoski KP, et al. Time constant of the cerebral arterial bed. Acta Neurochir Suppl. 2012;114:17–21.
10. Varsos GV, Richards H, Kasprowicz M, Budohoski KP, Brady KM, Reinhard M, et al. Critical closing pressure determined with a model of cerebrovascular impedance. J Cereb Blood Flow Metab. 2013;33:235–43.
11. Kasprowicz M, Czosnyka M, Soehle M, Smielewski P, Kirkpatrick PJ, Pickard JD, et al. Vasospasm shortens cerebral arterial time constant. Neurocrit Care. 2012;16:213–8.
12. Carrera E, Kim D-J, Castellani G, Zweifel C, Smielewski P, Pickard JD, et al. Cerebral arterial compliance in patients with internal carotid artery disease. Eur J Neurol. 2011;18:711–8.
13. Varsos GV, Budohoski KP, Czosnyka M, Kolias AG, Nasr N, Donnelly J, et al. Cerebral vasospasm affects arterial critical closing pressure. J Cereb Blood Flow Metab. 2015;35:285–91.
14. Varsos GV, Kolias AG, Smielewski P, Brady KM, Varsos VG, Hutchinson PJ, et al. A noninvasive estimation of cerebral perfusion pressure using critical closing pressure. J Neurosurg. 2015;123:638–48.
15. Carrera E, Kim D-J, Castellani G, Zweifel C, Czosnyka Z, Kasprowicz M, et al. What shapes pulse amplitude of intracranial pressure? J Neurotrauma. 2010;27:317–24.
16. Ambarki K, Baledent O, Kongolo G, Bouzerar R, Fall S, Meyer ME. A new lumped-parameter model of cerebrospinal hydrodynamics during the cardiac cycle in healthy volunteers. IEEE Trans Biomed Eng. 2007;54:483–91.
17. Czosnyka M, Smielewski P, Kirkpatrick P, Piechnik S, Laing R, Pickard JD. Continuous monitoring of cerebrovascular pressure-reactivity in head injury. Acta Neurochir Suppl. 1998;71:74–7.
18. Czosnyka M, Guazzo E, Whitehouse M, Smielewski P, Czosnyka Z, Kirkpatrick P, et al. Significance of intracranial pressure waveform analysis after head injury. Acta Neurochir. 1996;138:531–42.
19. Poulin MJ, Robbins PA. Indexes of flow and cross-sectional area of the middle cerebral artery using doppler ultrasound during hypoxia and hypercapnia in humans. Stroke. 1996;27:2244–50.
20. Valdueza JM, Balzer JO, Villringer A, Vogl TJ, Kutter R, Einhäupl KM. Changes in blood flow velocity and diameter of the middle cerebral artery during hyperventilation: assessment with MR and transcranial Doppler sonography. Am J Neuroradiol. 1997;18:1929–34.
21. Henriksen JH, Fuglsang S, Bendtsen F, Christensen E, Møller S. Arterial compliance in patients with cirrhosis: stroke volume-pulse pressure ratio as simplified index. Am J Physiol Gastrointest Liver Physiol. 2001;280:G584–94.
22. Panerai RB, Salinet ASM, Brodie FG, Robinson TG. The influence of calculation method on estimates of cerebral critical closing pressure. Physiol Meas. 2011;32:467–82.

23. Altman BjM. DG. Statistics notes: calculating correlation coefficients with repeated observations: part 1-correlation within subjects. BMJ. 1995;310:446.
24. Bland JM, Altman DG. Calculating correlation coefficients with repeated observations: Part 2-correlation between subjects. BMJ. 1995;310:633.
25. Varsos GV, Kasprowicz M, Smielewski P, Czosnyka M. Model-based indices describing cerebrovascular dynamics. Neurocrit Care. 2014;20:142–57.
26. Brothers RM, Zhang R. CrossTalk opposing view: the middle cerebral artery diameter does not change during alterations in arterial blood gases and blood pressure. J Physiol. 2016;594:4077–9.
27. Hoiland RL, Ainslie PN. CrossTalk proposal: The middle cerebral artery diameter does change during alterations in arterial blood gases and blood pressure. J Physiol. 2016;594:4073–5.
28. Djurberg HG, Seed RF, Price Evans DA, Brohi FA, Pyper DL, Tjan GT, et al. Lack of effect of CO_2 on cerebral arterial diameter in man. J Clin Anesth. 1998;10:646–51.
29. Serrador JM, Picot P, Rutt BK, Shoemaker JK, Bondar RL. MRI measures of middle cerebral artery diameter in conscious humans during simulated orthostasis. Stroke. 2000;31:1672–8.
30. Schreiber SJ, Gottschalk S, Weih M, Villringer A, Valdueza JM. Assessment of blood flow velocity and diameter of the middle cerebral artery during the acetazolamide provocation test by use of transcranial Doppler sonography and MR imaging. AJNR Am J Neuroradiol. 2000;21:1207–11.
31. Verbree J, Bronzwaer A-SGT, Ghariq E, Versluis MJ, Daemen MJAP., van Buchem MA, et al. Assessment of middle cerebral artery diameter during hypocapnia and hypercapnia in humans using ultra-high-field MRI. J Appl Physiol. 2014;117:1084–9.
32. Coverdale NS, Lalande S, Perrotta A, Shoemaker JK. Heterogeneous patterns of vasoreactivity in the middle cerebral and internal carotid arteries. Am J Physiol- Hear Circ Physiol. 2015;308:H1030–8.
33. Kim S-G, Harel N, Jin T, Kim T, Lee P, Zhao F. Cerebral blood volume MRI with intravascular superparamagnetic iron oxide nanoparticles. NMR Biomed. 2013;26:949–62.